^{222}Rn from interstitial waters by CH_4 bubbles (*18*). Our data suggest that a significant portion of the CH_4 released from Cape Lookout Bight sediments during the summer is derived from the fermentation of acetate to CH_4 in the sulfate-depleted sediments in the depth range from 8 to 35 cm.

FRANCIS J. SANSONE*
CHRISTOPHER S. MARTENS
University of North Carolina Marine Science Program, Chapel Hill 27514, and *Institute of Marine Sciences, Morehead City, North Carolina 28557*

References and Notes

1. G. E. Claypool and I. R. Kaplan, in *Natural Gases in Marine Sediments*, I. R. Kaplan, Ed. (Plenum, New York, 1974), pp. 99–139; D. E. Hammond, in *ibid.*, pp. 71–89; C. S. Martens and R. A. Berner, *Science* **185**, 1167 (1974); T. Whelan, *Estuarine Coastal Mar. Sci.* **2**, 407 (1974); R. O. Barnes and E. D. Goldberg, *Geology* **4**, 297 (1976); W. S. Reeburgh, *Earth Planet. Sci. Lett.* **28**, 337 (1976).
2. R. A. Mah, D. M. Ward, L. Baresi, T. S. Glass, *Annu. Rev. Microbiol.* **31**, 309 (1977); J. G. Zeikus, *Bacteriol. Rev.* **41**, 514 (1977).
3. A. J. B. Zehnder, in *Water Pollution Microbiology*, R. Mitchell, Ed. (Wiley, New York, 1978), pp. 349–376.
4. D. H. Ehhalt, *Tellus* **26**, 58 (1974).
5. C. S. Martens and J. V. Klump, *Geochim. Cosmochim. Acta* **44**, 471 (1980).
6. T. E. Cappenberg and R. A. Prins, *Antonie van Leeuwenhoek J. Microbiol. Serol.* **40**, 457 (1974).
7. M. R. Winfrey and J. G. Zeikus, *Appl. Environ. Microbiol.* **37**, 244 (1979).
8. C. S. Martens, *Science* **192**, 998 (1976); _____, G. W. Kipphut, J. V. Klump, *ibid.* **208**, 285 (1980). An aerial photograph of the field site was printed on the cover of the 18 April 1980 issue of *Science*.
9. F. J. Sansone and C. S. Martens, *Limnol. Oceanogr.* **23**, 349 (1978).
10. C. S. Martens, unpublished data.
11. J. V. Klump and C. S. Martens, *Geochim. Cosmochim. Acta* **45**, 101 (1981).
12. F. J. Sansone and C. S. Martens, *Mar Chem.*, in press.
13. The sediment porosity decreases from 0.94 to 0.87 cm^3 of interstitial water per cubic centimeter of whole wet sediment in the top 25 cm and remains approximately at the latter value to a depth of 50 cm.
14. F. J. Sansone, thesis, University of North Carolina at Chapel Hill (1980).
15. R. R. Christian and W. J. Wiebe, *Limnol. Oceanogr.* **23**, 328 (1978). Briefly, five to six samples were taken from each experiment with two to three of these used as abiotic ("killed") controls. We obtained samples of cores by inserting 3-ml plastic syringes with cutoff ends; these core samples were transferred to sterile 15-ml Vacutainer tubes flushed with O_2-free N_2. One milliliter of sterile, degassed, sulfate-free artificial seawater was added to each tube; these tubes were then Vortex-mixed and equilibrated for 30 minutes at the in situ temperature. An aqueous solution of labeled acetate (10 to 50 μl) was added anaerobically to each tube; the tubes were incubated for 5 minutes at the in situ temperature and then "killed" with acid formalin. Controls were "killed" before label had been added. Activity was recovered as follows: (i) $^{14}CO_2$ on phenethylamine-treated filter paper; (ii) $^{14}CH_4$ by the method of A. J. B. Zehnder, B. Huser, and T. D. Brock [*Appl. Environ. Microbiol.* **37**, 897 (1979)]; (iii) labeled particulate (including cellular) material; (iv) labeled water-soluble, but not ether-soluble, material; and (v) labeled ether-soluble material (that is, nonutilized substrate). Typically, 85 to 90 percent of the added label was recovered at the end of each experiment. Only the CH_4 and CO_2 production data are presented in this report.
16. Preliminary anaerobic sediment incubation experiments by one of us (F.J.S.), using Cape Lookout sediments, indicated immediate net CH_4 accumulation only in samples with initial in situ sulfate concentrations less than 1 m*M*.
17. By numerically integrating the area under the total CH_4 flux curve (Fig. 1A) and the apparent acetate turnover to CH_4 curve (Fig. 1B) over equal time intervals, one can compare the measured rate of CH_4 production in the top 5 cm of the CH_4 production zone with the measured flux out of the sediment during the given interval.
18. G. W. Kipphut and C. S. Martens, in preparation. A deficit in the concentration of the dissolved radioactive gas ^{222}Rn between 10 and 30 cm during the summer months results from in situ stripping of this gas from the sediment interstitial waters by CH_4 bubbles. This provides direct evidence for CH_4 production in, and transport from, this depth interval.
19. We thank G. Kipphut and P. Crill for help in the collection of samples. We also thank the staffs of the University of North Carolina Institute of Marine Sciences and the National Oceanic and Atmospheric Administration National Marine Fisheries Service Laboratory, Beaufort, N.C. We thank C. D. Taylor of Woods Hole Oceanographic Institution and M. B. Goldhaber of the U.S. Geological Survey, Denver, for critical remarks on an early version of this report. Research supported by NSF grants OCE78-09485 and OCE80-09245 (C.S.M.) and OCE78-09507 (F.J.S.) from the Marine Chemistry Program, Oceanography Section.
* Present address: Department of Oceanography, University of Hawaii, Honolulu 96822.

12 September 1980; revised 24 November 1980

Membrane Conductance and Action Potential of a Regenerating Axonal Tip

Abstract. *The electrical membrane properties of axotomized and regenerating giant axons from the nerve cord of the cockroach* Periplaneta americana *were studied. Immediately after axotomy there was a decrease in resting potential, input resistance, and action potential amplitude near the cut end. This decrease was followed by the disappearance of the sodium-dependent action potential; an increase in the resting membrane conductance to K^+, Na^+, and Ca^{2+}; and the appearance of a calcium-dependent action potential.*

In many neurons, axonal transection leads to changes in morphology, metabolism, and membrane properties (*1*). Changes in input resistance, resting and action potentials, afterhyperpolarization, and excitability have been demonstrated in the somata and in dendrites remote from the site of transection (*2*). At the site of transection, a large injury potential and loss of excitability have been demonstrated (*3*). Recovery takes place gradually within a few days (*3*). Several investigators have suggested that ionic fluxes through the injured region and the ensuing change in intracellular ion composition may trigger the degenerative and regenerative responses. Membrane properties at the site of transection must

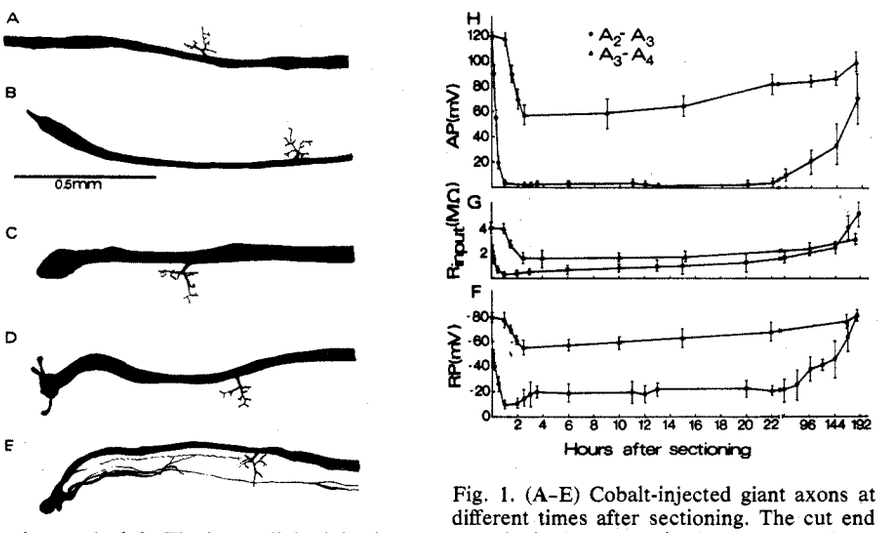

Fig. 1. (A–E) Cobalt-injected giant axons at different times after sectioning. The cut end points to the left. The intracellular injections were made, in the connective between ganglia A_3 and A_4. (A) A normal giant axon [number II in (*17*)] emits a neurite in ganglion A_3 (in the middle of the figure). (B) Twenty-four hours after sectioning, the cut end was sealed. (C) Forty-eight hours after sectioning, the cut end showed a swelling. (D) Seven days after sectioning, sprouts emerged from the bulging end. (E) Twenty-six days after sectioning, the sprouts elongated in a retrograde direction. Some variability in the length, shape, and number of sprouts has been observed in different preparations. Despite this, the figure is representative of the sequence of growth. (F–H) Membrane properties of the giant axons at different times after axotomy and at different distances from the cut end of the axon. Values of (F) resting potential, (G) input resistance, and (H) action potential amplitude rapidly fell during the first hour and then gradually recovered to normal by 8 to 10 days after sectioning. Intracellular recordings were made 0.2 to 0.3 mm caudal to the cut end, anterior to ganglion A_3 (closed circles), and more distant from it, close to ganglion A_4 (triangles), 5 ± 0.5 mm from the cut end. Each value is a mean ± standard deviation of results taken from 5 to 12 preparations. Input resistance was measured at membrane potentials more negative than −90 mV (*7*).

0036-8075/81/0213-0709$00.50/0

play an important role in regulating the ionic fluxes and possibly thereby the responses of the neuron to injury. Except for the study of Borgens *et al.* (*3*), in which the specific ionic fluxes through a transected lamprey cord were determined by extracellular current recordings, this question had not been investigated.

We examined passive and active membrane properties at various distances from the site of axonal transection during the period of recovery and regeneration. The giant axon system of the cockroach *Periplaneta americana* (*4*) allows intracellular recording near the cut end, so that membrane properties can be studied as a function of time after axotomy and as a function of distance from the cut end. The normal membrane properties are well characterized in this system (*5*). The axons, which are 20 to 40 μm in diameter and 2 to 3 cm long, arise from somata located at the last abdominal ganglion (A_6). They traverse the ventral nerve cord and emit one to seven neurites in each ganglion (*6*). In preparation for transection of the giant axons, adult cockroaches were anesthetized with CO_2. The ventral nerve cord was cut between ganglia A_2 and A_3 by inserting fine scissors between the sternites. The animals recovered from anesthesia quickly and were able to walk and eat fairly normally. Most animals survived for months after this surgical procedure.

To study short-term effects of axotomy, we isolated the nerve cord and cut it while we were recording intracellularly from one of its axons. For the study of long-term changes, the nerve cord was cut in situ and animals were killed at various times thereafter.

The morphology of the proximal region of the giant axon (the section connected to the soma) was studied by intracellular injection of cobalt ions (*6*) between A_3 and A_4 (Fig. 1). No cobalt precipitate could be detected if the injection was made 1 to 4 hours after axotomy. We interpret this result to indicate leakage of Co^{2+} through the open cut end. Staining intensity gradually increased as the interval between axotomy and injection was prolonged. A sharp boundary at the cut end was seen 20 to 24 hours after axotomy, an indication that an efficient barrier to Co^{2+} was formed by this time (Fig. 1B). By 48 hours, the cut end bulged, and by 7 days, three to five sprouts had emerged (Fig. 1, A to D). The sprouts gradually elongated in a retrograde direction (Fig. 1E) (*7*). These changes took place within 0.2 mm of the cut end; we could detect no changes in the morphology of the rest of the axon.

Resting potential and input resistance of the fibers were studied by conventional electrophysiological techniques. The following changes occurred 0.2 to 0.4 mm caudal to the cut end, a region anterior to ganglion A_3. This region roughly corresponds to the bulged sections in the axotomized giant axon. During the first 1 to 2 hours, the resting potential was reduced from -80 to -10 mV (Fig. 1F). The input resistance (*8*) dropped from ~ 4 to ~ 0.3 megohm (Fig. 1G). At the same time, the amplitude of the action potential produced by stimulation of the connectives between ganglia A_5 and A_6 was reduced from 120 mV to 1 to 4 mV (Fig. 1H). The rate of these changes was greatest during the first 5 minutes when all values fell by about 50 percent. These values continued to drop at a slower pace during the first hour. It is reasonable to assume that the changes seen during the first 5 minutes resulted from exposure of the interior of the axon to the extracellular medium. The progressive changes that appeared later may have resulted from continuous diffusion of ions along their gradients. The resting potential repolarized slightly between 2 and 4 hours after axotomy, but there was no further recovery during the ensuing 48 hours. Thereafter there was a gradual recovery of membrane potential until day 10 (Fig. 1F), when normal resting potential values were achieved.

The input resistance began to recover after about 2 hours and was normal about 8 days after axotomy (Fig. 1G), but then rose above normal between 10 and 19 days (*9*). Normal values were again reached at 22 to 24 days (not shown in Fig. 1). During the first 48 hours, the propagated action potential failed to reach the cut end, and only a small (5 to 10 mV) decremental potential was recorded. Impulse conduction gradually recovered and was normal on about day 9 (Fig. 1H).

Similar changes in membrane properties were seen at a distance from the cut. However, the effects of axotomy on axonal membrane properties were more pronounced close to the site of injury than further away. Thus, at ganglion A_4 (mean $\pm$ standard deviation of 5.5 ± 0.5 mm from the cut end in seven experiments), the changes were smaller (Fig. 1, F to H), and at ganglion A_5 (12 ± 0.7 mm from the cut end in seven experiments),

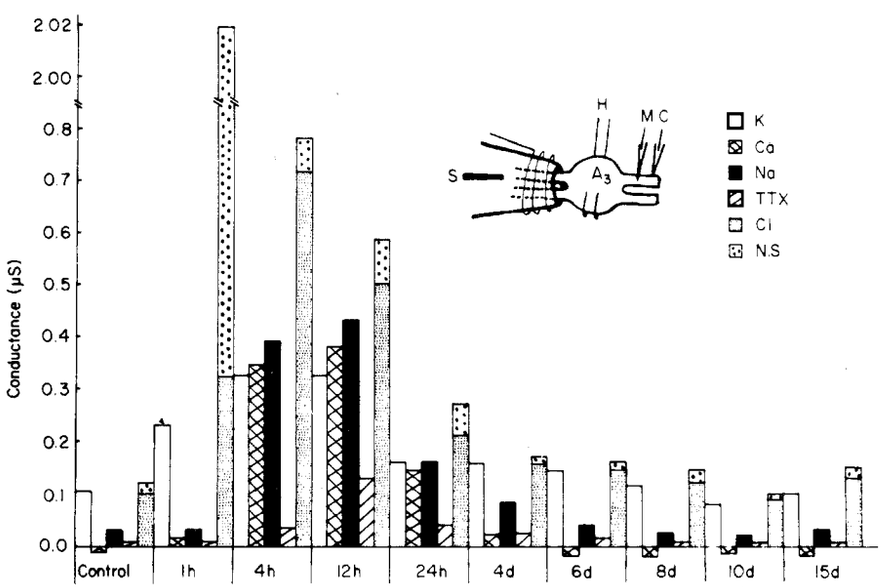

Fig. 2. Resting ionic conductances measured at the tip of a giant axon at different times after sectioning. For procedure, see text. The bars indicate the change (decrease) in membrane conductance after sequential elimination of specific ionic conductances (see text). Note, however, that in the control, reduction in the Ca^{2+} concentration resulted in an increase in membrane conductance (downward deflection), probably due to indirect effects on conductances of other ions. One hour to 4 days after sectioning, conductance was decreased after removal of Ca^{2+}, indicating an increasing fraction of Ca^{+} conductance from the total membrane conductance. After 6 days, removal of Ca^{2+} produced the same effect as in the control. (Inset) Experimental setup. The nerve cord, from the cercal nerve to the caudal base of ganglion A_3, was sucked into a suction electrode *S*. This electrode was used to pass current and hyperpolarize the membrane to about -80 mV (the normal resting potential) or more negative values. Input resistance was measured with the intracellular electrode (*M*), which was used for passing current and for recording voltage changes (WP-I microprobe system). The control electrode (*C*) was used for measuring current flow directly from *S* to the indifferent electrode in the bath. Membrane potential (monitored by *M*) was changed by injection of current pulses 1 to 3 minutes in duration. Hook electrodes (*H*) were used to stimulate the nerve cord with short pulses to produce action potentials. *TTX*, tetrodotoxin; *NS*, nonspecific.

membrane properties were almost normal (not shown).

During the process of recovery, the membrane at the cut end progresses from a leaky, nonselective state to a new ionic selectivity and then gradually returns to normal. The resting membrane conductance for Na^+, K^+, Ca^{2+}, and Cl^- was determined near the cut end of the axon at different times after the connectives were sectioned. Values of the membrane conductance to each of these ions was determined in the following way. The total conductance, g_{total} (Fig. 2) was measured in normal physiological solution (*10*) as $1/R_{input}$. Potassium conductance g_K is defined, in this case, as the difference between g_{total} and the conductance in the presence of $10^{-3}M$ 4-aminopyridine (4-AP) (*11*). "Calcium conductance," g_{Ca}, was then computed as the difference between the conductance value measured after addition of 4-AP and after reduction of extracellular Ca^{2+} concentration from 9 to 0.5 m*M* (*12*). Sodium conductance was measured as the difference between the value obtained after reduction of external Ca^{2+} and after replacing all extracellular sodium ions by tris [tris(hydroxymethyl)-aminomethane]. Chloride conductance was determined from the difference between g_{total} and the conductance measured after propionate was substituted for chloride. The remaining conductance, after all of these conductances were subtracted from g_{total}, is defined here as a nonspecific conductance g_{NS}. These changes were reversed when normal ionic composition was restored.

In normal giant axons resting conductance is mostly attributable to g_K; g_{Cl} and g_{Na} are low, and g_{Ca} is negligible (Fig. 2). During the first hour after axotomy, the axonal tip became highly permeable to all ions: g_{NS} was 78 percent of total membrane conductance. This value probably represents the shunt by the open end. At 4 hours after axotomy and for a period of at least 24 hours, all ionic conductances increased; g_{Na} and g_{Ca} increased to 4 to 20 times normal, respectively, and g_K and g_{Cl} increased to twice normal. Membrane selectivity and conductances gradually recovered and were normal at 8 days.

Immediately after axotomy, the Na^+-dependent action potential evoked by stimulating the connective between A_5 and A_6 did not actively propagate into the region near the cut end. This failure resulted from membrane depolarization and sodium inactivation (*13*). Hyperpolarization (Fig. 2, inset) of the membrane to −80 mV restored full invasion of the action potential, and it became possible to evoke a full-sized action potential with direct intracellular stimulation. However, between 3 and 48 hours after axotomy it was impossible to restore the invasion of an action potential into the region of the cut end, even with prolonged hyperpolarization. Similarly, it was impossible to evoke a full action potential with direct intracellular stimulation at this time. Full recovery occurred about 8 days after axotomy.

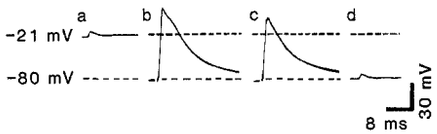

Fig. 3. Demonstration of Ca^{2+}-dependent action potentials 48 hours after axotomy. The dotted line represents the resting potential at the beginning of the experiment (−21 mV); (panel a) stimulation of the cord produced a small response; (panel b) after addition of 4AP and substitution of 214 m*M* tris for sodium, the membrane hyperpolarized to −80 mV and stimulation produced an overshooting action potential; (panel c) this action potential was not blocked by $10^{-7}M$ tetrodotoxin; (panel d) addition of 9 m*M* Co^{2+} abolished the action potential, and only a small response remained. Washing reversed these changes at each stage.

The Ca^{2+}-dependent action potential is shown in the experiment of Fig. 3. Forty-eight hours after axotomy, the resting membrane potential was −21 mV, and stimulation of the connective produced a minor response (Fig. 3, trace a). Hyperpolarization of the membrane to between −60 and −80 mV did not alter the response. After the addition of 4-AP and replacement of sodium ions by tris (*14*), the membrane potential was repolarized to −80 mV, and the input resistance increased. Under these conditions, stimulation of the connectives produced an overshooting action potential (Fig. 3, trace b). Addition of $10^{-7}M$ tetrodotoxin to this solution produced only a slight reduction of the action potential amplitude (Fig. 3, trace c). This action potential was blocked by the addition of 9 m*M* cobalt, and only a small response remained (Fig. 3, trace d). The amplitude of the action potential was dependent on the external Ca^{2+} concentration. In a plot of amplitude versus the logarithm of the extracellular calcium concentration, the slope of the line was 22.8 (between 3.6 to 36 m*M* extracellular Ca^{2+}). This value is in close agreement with the prediction from the Nernst equation. The Ca-dependent action potential appeared first about 7 hours after axotomy and disappeared about 60 hours after axotomy; Ca^{2+}-dependent action potentials were recorded only near the cut end anterior to ganglion A_3. In more caudal regions, the normal Na^+-dependent action potential was preserved throughout this period. Similar experiments in intact cords showed that the Ca^{2+}-dependent action potential was blocked by tetrodotoxin and was insensitive to Co^{2+}.

We have shown that the membrane properties at the regenerating tip of an axon differ from those of the normal membrane. Electrophysiological methods do not allow precise localization of the membrane responsible for these properties, since the space constant of the cut axon cannot be determined accurately. However, it is safe to assume that the changes occurred 0.2 to 0.4 mm from the cut end (rostral to ganglion A_3).

The events seen after axotomy can be divided into four stages: (i) nonspecific shunting and mixing of extracellular and intracellular ions and molecules; (ii) formation of a barrier to cobalt and possibly to large molecules; (iii) differentiation of the membrane at or near the cut end to show resting selective ionic conductances different from normal and a Ca-dependent action potential; and (iv) complete recovery of the ionic conductances to normal. It should be emphasized that this recovery was measured at a recording site just proximal to the transection and therefore cannot be extended with certainty to the growing tip, now at some distance from the recording site. In fact, calculations of membrane input resistance at the recording site (*9*) suggest that the growing tip retains the new or modified membrane properties.

We have described changes in time and space of axonal membrane properties after axotomy. It is not clear whether the new ionic conductances seen near the region of the outgrowing tip are produced by alteration of previously existing ionic channels or whether new channels are introduced (or activated) near the cut end. It is also not possible to distinguish at this stage whether these new ionic properties are a consequence of the insertion of new growing membrane or a requirement for the insertion of new membrane. However, our results support the general hypothesis of Llinas (*15*), which links a local increase in the intracellular Ca^{2+} concentration to the growth of a given region of a neuron. It is also interesting that 24 to 48 hours after axotomy, the membrane properties at the site of transection resemble the properties of some embryonic tissues (*16*).

HAMUTAL MEIRI
MICHA E. SPIRA, ITZAK PARNAS
Neurobiology Unit, Life Sciences Institute, Hebrew University, Jerusalem, Israel

References and Notes

1. A. R. Lieberman, in *Essays on the Nervous System*. R. Bellairs and E. G. Gray, Eds. (Clarendon, Oxford, 1974), pp. 71-105; R. P. Vera, B. Grafstein, R. A. Ross, *Exp. Neurol.* **64**, 649 (1979).
2. M. Kuno and R. Llinas, *J. Physiol. (London)* **210**, 807 (1970); M. Kuno, Y. Miyata, E. J. Munoz-Martinez, *ibid.* **140**, 725 (1974); R. M. Pitman, C. D. Tweedle, M. J. Cohen, *Science* **178**, 507 (1972); R. M. Pitman, *J. Physiol. (London)* **247**, 511 (1975).
3. R. B. Borgens, L. F. Jaffe, H. J. Cohen, *Proc. Natl. Acad. Sci. U.S.A.* **77**, 1209 (1980); J. C. Eccles, K. Krnjevic, R. Miledi, *J. Physiol. (London)* **145**, 214 (1959); B. G. Cragg and P. K. Thomas, *ibid.* **171**, 164 (1964); G. Czeh, N. Kudo, M. Kudo, *ibid.* **270**, 165 (1977).
4. R. D. Farley and N. W. Milburn, *J. Insect Physiol.* **15**, 457 (1969); M. E. Spira, I. Parnas, F. Bergman, *J. Exp. Biol.* **50**, 615 (1969).
5. T. Narahashi, *Comp. Biochem. Physiol.* **19**, 759 (1966); I. Parnas, M. E. Spira, R. Werman, F. Bergman, *J. Exp. Biol.* **50**, 635 (1969); I. Parnas and D. Dagan, in *Advances in Insect Physiology*, J. W. L. Beament, J. E. Treherne, V. B. Wigglesworth, Eds. (Academic Press, New York, 1971), vol. 8, pp. 96-144; Y. Pichon, in *Insect Neurobiology*, J. E. Treherne, Ed. (North-Holland, Amsterdam, 1974), pp. 93-117; M. E. Spira, Y. Yarom, I. Parnas, *J. Neurophysiol.* **39**, 882 (1976).
6. Intracellular cobalt injections were made according to the technique developed by R. M. Pitman, C. D. Tweedle, and M. J. Cohen [*Science* **176**, 412 (1972)] and repeated by M. Castel, M. E. Spira, I. Parnas, and Y. Yarom [*J. Neurophysiol.* **39**, 900 (1976)].
7. The reason for this "erroneous" growth of the axons is unknown. However, it must be pointed out that during nerve cord sectioning the two cut ends are separated from each other.
8. The input resistance of the giant axons is voltage-dependent, showing delayed rectification at values positive to −75 mV. Therefore, the values were measured at membrane potential values below −90 mV [M. E. Spira *et al.* (*5*)].
9. It is expected that if the membrane properties of the sealed tip are normal then the input resistance measured at this site should be almost twice normal [J. J. B. Jack, D. Nobel, R. W. Tsein, in *Electric Current Flow in Excitable Cell* (Clarendon, Oxford, 1975), pp. 67-72]. We have computed the expected input resistance of the cut axon, taking into account the geometry of the axon 10 to 19 days after axotomy, using Rall's approximations [W. Rall, *Ann. N.Y. Acad. Sci.* **96**, 1071 (1962)]. In our computations we assumed normal membrane resistance for the sprouts. The calculations show that the input resistance is expected to be larger than that in Fig. 1G. This discrepancy indicates that at least part of the membrane of the sprouts had a lower resistance than normal.
10. Normal solution contained: NaCl, 214 n*M*; $CaCl_2$, 9 n*M*; tris, 2 m*M*; and glucose, 1 mg/ml at *p*H 7.4.
11. 4-Aminopyridine is a selective blocker of potassium channels in the giant axons of the cockroach [Y. Pichon, in *Prospective in Experimental Biology*, P. Spencer Davies, Ed. (Pergamon, Oxford, 1976), pp. 297-312].
12. We could not replace all of the Ca^{2+} as the axons deteriorated rapidly. It should be emphasized that this method only allows a comparison of the effects of removal of Ca^{2+} on membrane conductance at various times after axotomy. Extracellular Ca^{2+} is known to affect the conductance of other ions [K. Krnjevic and A. Lisiewicz, *J. Physiol. (London)* **225**, 363 (1972); R. W. Meech, *Comp. Biochem. Physiol. A* **42**, 493 (1972); C. B. Heyer and H. D. Lux, *J. Physiol. (London)* **262**, 319 (1976)].
13. H. L. Hodgkin and A. F. Huxley, *J. Physiol. (London)* **116**, 497 (1952).
14. This was done by replacing all sodium ions in the physiological solution (240 m*M*) by tris. Maximal change in input and resting potential produced by this treatment was obtained after 10 to 15 minutes of washing at a rate of 2 to 3 ml/min.
15. R. Llinas, in *Fourth Study Program*, F. O. Schmitt and F. G. Worden, Eds. (MIT Press, Cambridge, Mass., 1979), pp. 555-571; _____ and M. Sugimori, *Prog. Brain Res.* **51**, 323 (1979).
16. N. C. Spitzer, *Annu. Rev. Neurosci.* **2**, 363 (1979).
17. C. L. Harris and T. Smyth, *Comp. Biochem. Physiol. A* **40**, 295 (1971).

18. Supported by grants from the Israel Commission for Basic Research, the Israel Academy of Sciences and Humanities, and the United States-Israel Binational Science Foundation (No. 1829).

10 April 1980; revised 28 July 1980

Gap Junctional Conductance Is a Simple and Sensitive Function of Intracellular *p*H

Abstract. *The* p*H of the cytoplasm* (pH_i) *measured with* p*H-sensitive microelectrodes in cleavage-stage blastomeres of amphibian* (Ambystoma) *and teleost* (Fundulus) *embryos is about 7.7. In electrotonically coupled cell pairs, junctional conductance is rapidly and reversibly reduced by acidification of the cytoplasm. The relation between junctional conductance and* pH_i *is the same for increasing and decreasing* p*H and is independent of the rate of change over a wide range. The relation is well fitted by a Hill curve with* K = 50 n*M* (p*K* = 7.3) *and* n = 4 *to* 5. *The closure of gap junction channels at low* pH_i *appears to be a cooperative process involving several charged sites. The absence of hysteresis and identity of effects for fast and slow* pH_i *changes implies that protons act directly on the channel macromolecules and not through an intermediate in the cytoplasm.*

Gap junctions are close appositions of cell membranes where polygonal aggregates of intramembrane particles are in one-to-one correspondence in the apposed cells (*1*). The particles are composed of proteins that form hydrophilic channels connecting the cytoplasms of the two cells. The channels permit passage of molecules whose maximum molecular weight is near 1000 and whose diameter can be somewhat greater than 1.0 nm (*1, 2*). In excitable cells, gap junctions mediate intercellular transmission of electrical signals. In tissues that are not excitable, the junctions allow intercellular spread of nutrients and metabolites and may also transmit chemical messages (*3*). For both excitable and inexcitable cells, treatments that depress junctional conductance would be expected to disturb coordinated physiological functioning of the tissue.

In previously reported experiments on various tissues, exposure of coupled cells to saline containing high CO_2 concentrations reduced electrotonic coupling (*4-7*). Exposure of coupled cells to membrane-impermeant acids was without effect on coupling, suggesting that the effect of CO_2 was mediated by acidification of the cytoplasm. In some experiments, cytoplasmic acidification by CO_2 was confirmed by direct measurement of intracellular *p*H (*p*H_i) (*5, 6*). Although uncoupling was shown to be at least partially due to decreased junctional conductance, the interpretation of most of these experiments was complicated by failure to measure junctional conductance directly (*4, 6*).

We now report that *p*H_i and junctional conductance are strictly related during cytoplasmic acidification with weak acids. This relation suggests a direct interaction of protons with the macromolecules that comprise the junctional channels. The same treatments produce changes in nonjunctional conductance that are not simple or consistent functions of *p*H_i. The coupling coefficients (*8*), which depend on the conductances of both junctional and nonjunctional membranes, are therefore not strictly dependent on *p*H_i.

Embryos from *Ambystoma mexicanum* (late blastula stage) and *Fundulus heteroclitus* (32- to 64-cell stage) were used for these studies. Single cells or cell pairs were mechanically dissociated in saline (*9*) containing up to 0.05 percent colchicine to inhibit mitosis. Within 30 minutes after the single cells were reassociated as pairs, a steady-state level of coupling developed. Each cell of a pair was penetrated with separate current and voltage microelectrodes (3*M* KCl, 5 to 20 megohms). In addition, one cell of each pair was penetrated with a Thomas-type recessed-tip *p*H microelectrode (*10*). Current pulses were passed alternately into each cell; measurements of input and transfer resistances allowed calculation of the junctional conductance (g_j) and of the nonjunctional conductances of the two cells (g_1 and g_2) by application of the π-*t* transform (*11*). Pulses were sufficiently brief that the voltage dependence of g_j in *Ambystoma* (*12*) could be neglected.

An experiment typical of those performed on pairs of blastomeres is shown in Fig. 1. The coupling coefficients for cell pairs were generally 0.8 to 0.9 at normal *p*H_i [*Ambystoma*: *p*H_i = 7.75 ± 0.06 standard deviation (S.D.) (*13*), *N* = 9; *Fundulus*: *p*H_i = 7.67 ± 0.06 S.D., *N* = 9]. Brief application of physiological saline equilibrated with 100 percent CO_2 (arrows, Fig. 1, top) decreased the internal *p*H. The coupling decreased and then dis-

0036-8075/81/0213-0712$00.50/0